



Optimum load computation of a piezoelectric-based energy harvester

Cálculo de la carga óptima de un sistema de cosecha basado en el efecto piezoeléctrico

Andrés Felipe Gomez-Casseres ¹

Fecha de Recepción: 30 de enero de 2023

Fecha de Aceptación: 15 de mayo de 2024

Cómo citar: Andrés Felipe Gomez-Casseres E. (2022). Optimum load computation of a piezoelectric-based energy harvester. *Tecnura*, 28(79), 53-65. <https://doi.org/10.14483/22487638.22164>

ABSTRACT

Objective: Maximum power extraction from piezoelectric energy harvesters is of key importance in the development of various current technologies. However, direct use of the maximum power transfer theorem on this type of energy harvester produces unstable and non-causal load models, which prevent its synthesis through a power electronic circuit and reduce the power available for the application's specific hardware. This article presents the computation of a causal and stable transfer function that approximates the maximum power extraction load of a linear piezoelectric harvester.

Methodology: Such a model is obtained using the Particle Swarm Optimization (PSO) algorithm, selected due to the simplicity of its implementation. In this study, a variation of the original algorithm is used to include the stability constraints.

Results: The algorithm was employed to obtain 7th, 8th, 16th, and 20th-degree models to evaluate the impact of model complexity on the obtained objective function values. The minimum cumulative square error resulted in an objective function value of approximately $6 \cdot 10^{-7} \Omega^{-2}$, attained by the 7th-degree model.

Conclusions: A stable and causal system model was obtained through a PSO implementation. Results suggest a low dependence of the minimum objective function value on increasing model degrees. Nevertheless, the best model matched the degree of the admittance transfer function. Finally, the implementation of the unconstrained PSO algorithm obtained better results, suggesting that a different optimization algorithm can attain better results.

Financing: This study was funded by the Corporación Nacional de Educación Superior CUN.

Keywords: Maximum power transfer theorem, optimum load, piezoelectric energy harvesting, particle swarm optimization.

¹Candidato a Magister en Ingeniería Electronica de la Pontificia Universidad Javeriana, Ingeniero Electronico de la Universidad Distrital Francisco Jose de Caldas. Docente Asistente en la Corporacion Unificada de Educacion Superior CUN Bogota Colombia

Email: andres_gomezcasseres@cun.edu.co

RESUMEN

Objetivo: La máxima extracción de potencia de los sistemas de cosecha de energía basados en el efecto piezoeléctrico es crucial para el desarrollo de diversas tecnologías actuales. Sin embargo, el uso directo del teorema de transferencia de máxima potencia en este tipo de captadores de energía produce modelos de carga inestables y no causales, que impiden su síntesis a través de un circuito electrónico de potencia y reducen la potencia disponible para el hardware específico de la aplicación. En este artículo, se presenta el cálculo de una función de transferencia causal y estable, que aproxima la máxima extracción de potencia de un cosechador piezoeléctrico lineal.

Metodología: Dicho modelo se obtiene mediante el algoritmo de Optimización por Enjambre de Partículas (PSO), seleccionado por su sencillez de implementación. En este estudio, se utiliza una variación del algoritmo original para incluir las restricciones de estabilidad.

Resultados: El algoritmo se empleó para obtener modelos de 7°, 8°, 16° y 20° grado para evaluar el impacto de la complejidad del modelo en los valores de la función objetivo obtenidos. El mínimo error cuadrático acumulado alcanzó un valor de la función objetivo de aproximadamente $6 \cdot 10^{-7} \Omega^{-2}$, alcanzado por el modelo de 7° grado.

Conclusiones: Se obtuvo un modelo estable y causal mediante una implementación de PSO. Los resultados sugieren una baja dependencia del valor mínimo de la función objetivo con el aumento de complejidad del modelo. No obstante, el mejor modelo coincidió con el grado de la función de transferencia de la admitancia. Finalmente, la implementación del algoritmo PSO sin restricciones produjo mejores resultados, sugiriendo que un algoritmo de optimización diferente puede alcanzar mejores resultados.

INTRODUCTION

Energy Harvesting (EH) has been demonstrated to be a promising technology that provides energy to low-power electronics when other, more traditional, methods cannot be used due to cost or reasons of access (Safaei *et al.*, 2019). The scavenging of the energy present in the surrounding environment has led to important advancements in areas like the Internet of Things (IoT), Wireless Sensor Networks (WSN), and systems in hazardous or hard-to-reach environments. In these and many other applications, due to its high output power density, Piezoelectric Energy Harvesting (PEH) serves as an interesting alternative as the new standard power generation system when vibrations or mechanical deformations are present.

Despite its high output power compared to other EH technologies, the generated power from PEH is very sensitive to frequency changes in mechanical excitation. This is because the piezoelectric element is commonly mounted on a glass-fiber beam and, to increase the output power, the system parameters are selected to obtain a highly peaked frequency response. This improves the power obtained when used in applications with very stable and deterministic excitation, but it also prevents energy scavenging in applications with intermittent or stochastic deformations (Uchino, 2018). This

problem is exacerbated by the lack of electronic circuits capable of harvesting the maximum available energy from the linear PEH at every possible extraction frequency (Todaro *et al.*, 2017).

To overcome the problem of harvesting energy at every possible frequency, it is mandatory that the electronic circuit that performs this task synthesize the optimum load of the PEH (Bowden *et al.*, 2015; Cammarano *et al.*, 2014; Ocalan *et al.*, 2017; Uchino, 2018). Given the dependency of the PEH impedance on the number of resonant frequencies and the geometry of the PEH, its computation could become very complex; this complexity is further compounded if an optimized geometry is used (Yang & Tang, 2009). Therefore, computing the optimum load becomes a rather intricate problem. Moreover, when the impedance of the PEH is available, the optimum load model obtained from the direct application of the Maximum Power Transfer Theorem (MPTT) can suffer from causality and instability issues, preventing straightforward implementation.

In this study, an alternative method based on the solution of an optimization problem to approximate the optimum load of a PEH is presented. This method guarantees the maximum power extraction from a PEH at several extraction frequencies, while producing an implementable model to control the output PEH current needed to emulate such a load by an electronic circuit.

PEH EQUIVALENT CIRCUIT

Figure 1 shows the equivalent circuit of a PEH, proposed by Yang (2009). This circuit is composed of two subcircuits that model the mechanical and electrical behavior of the PEH. The mechanical subcircuit is formed by k RLC circuits, in series with their respective voltage source v_k , connected in parallel through k ideal transformers. The RLC circuits model the mechanical behavior, in terms of stresses and deformations, of the PEH, while the transformers model the coupling between mechanical and electrical phenomena. Each k^{th} subcircuit represents a resonance of the PEH. Moreover, the electrical subcircuit is formed by the intrinsic capacitance of the piezoelectric material, C_p .

To calculate the optimum load of the PEH, the source admittance must be obtained. This quantity is presented in equation (1), where $s = j\omega$ and the transformer gain is computed as the number of turns on the mechanical side over the same number on the electrical side of the equivalent circuit. Furthermore, in Table 1, the component values for the first three resonant frequencies obtained by (Yang & Tang, 2009) are presented. With these values, the frequency response of the source admit-

tance of the PEH is presented in Figure 2. It should be pointed out that, unlike the second and the third resonant frequencies, which exhibit capacitive behaviors, the PEH displays an inductive behavior, represented by a negative phase, at the first resonance. This unexpected result proves that the second term of equation (1), which models the mechanical response, plays a major role in defining the output admittance.

$$Y_s = sC_e + \sum_{i=1}^k \frac{sN_i^2}{s^2L_i + sR_i + 1/C_i} \quad (1)$$

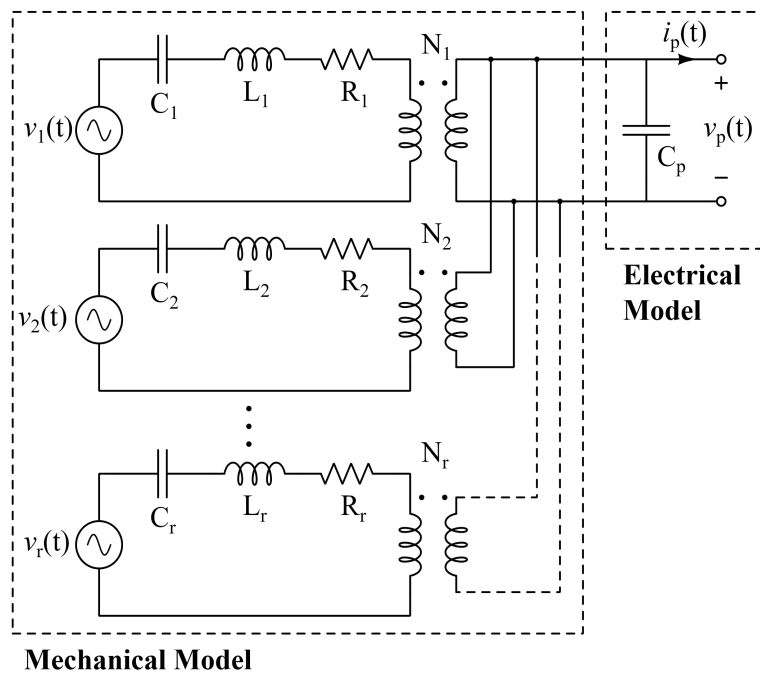


Figure 1. Equivalent electrical model of the PEH presented in (Yang & Tang, 2009)

Optimum Load through direct MPTT

Substituting the values presented in Table 1 on equation (1) and computing its complex conjugate, the optimum load of the PEH is obtained and presented in equation (2). This transfer function represents the optimal relation between the output current and voltage for obtaining the maximum power extraction from the PEH. Two major problems presented by the computed load admittance are its instability, given that its poles, which are $171,78 \pm 5505,48j$, $28,934 \pm 2096,83j$, $3,4683 \pm 412,59j$, have positive real values, and that equation (2) is a not proper transfer function. In this regard, although the unsuitability of the load admittance can be solved by adding additional high-frequency poles

while maintaining its low-frequency behavior, the instability problem makes the implementation of equation (2) impossible.

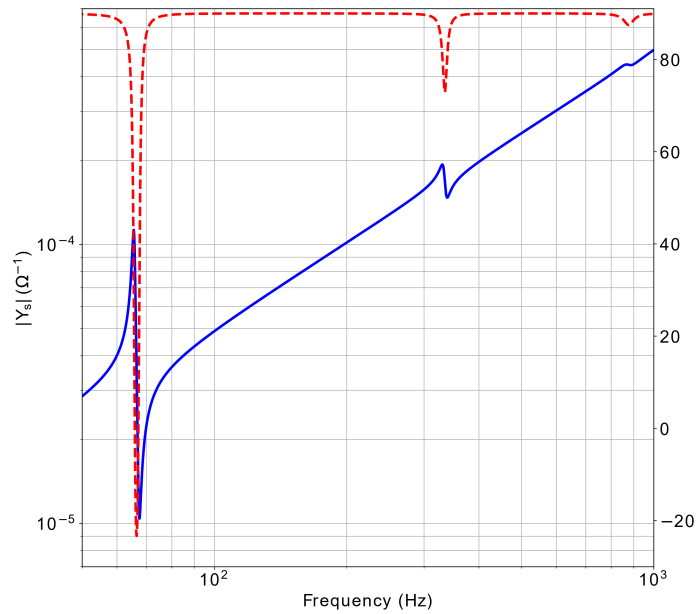


Figure 2. Source admittance at the output port (blue: magnitude response and red: phase response) of the PEH presented in (Yang & Tang, 2009).

Table 1. Piezoelectric Model Parameters and Optimal Load Values

Parameter	1 st Resonant Frequency	2 nd Resonant Frequency	3 rd Resonant Frequency
f_r	66.505 Hz	334.409 Hz	876.822 Hz
C_r	5,874 μ F	227.4 nF	32.96 nF
L_r	1 H	1 H	1 H
R_r	6,9366 Ω	57,868 Ω	343,56 Ω
N_r	0.0267198	0.0541673	0.0817594
Y_{opt}	29,67 + 12,75j μ S	49,74 161,465j μ S	– 19,46 – 440,3j μ S
L_{opt}	32.4787 nF	2.9493 H	0.4122 H
R_{opt}	31,781K Ω	20,116 K Ω	51,377 K Ω

$$Y_L = \frac{-3,52 \cdot 10^{-27} s^7 + 1,44 \cdot 10^{-24} s^6 - 1,24 \cdot 10^{-19} s^5 + 1,27 \cdot 10^{-17} s^4 - 4,98 \cdot 10^{-13} s^3 + 5,37 \cdot 10^{-12} s^2 - 8,51 \cdot 10^{-8} s}{4,4 \cdot 10^{-20} s^6 - 1,8 \cdot 10^{-17} s^5 + 1,54 \cdot 10^{-12} s^4 - 1,57 \cdot 10^{-10} s^3 + 6,14 \cdot 10^{-6} s^2 - 6,52 \cdot 10^{-5} s + 1} \quad (2)$$

Given the problems outlined, a common approach found in the literature is to load the PEH with a single-frequency optimum admittance. This approach uses a simple load admittance to achieve MPTT at a single resonant frequency. The optimum admittances for each resonant frequency, together with the circuit values that implement them, are presented in Table 1. It should be noted that the two components used to implement the optimum admittance are connected in parallel.

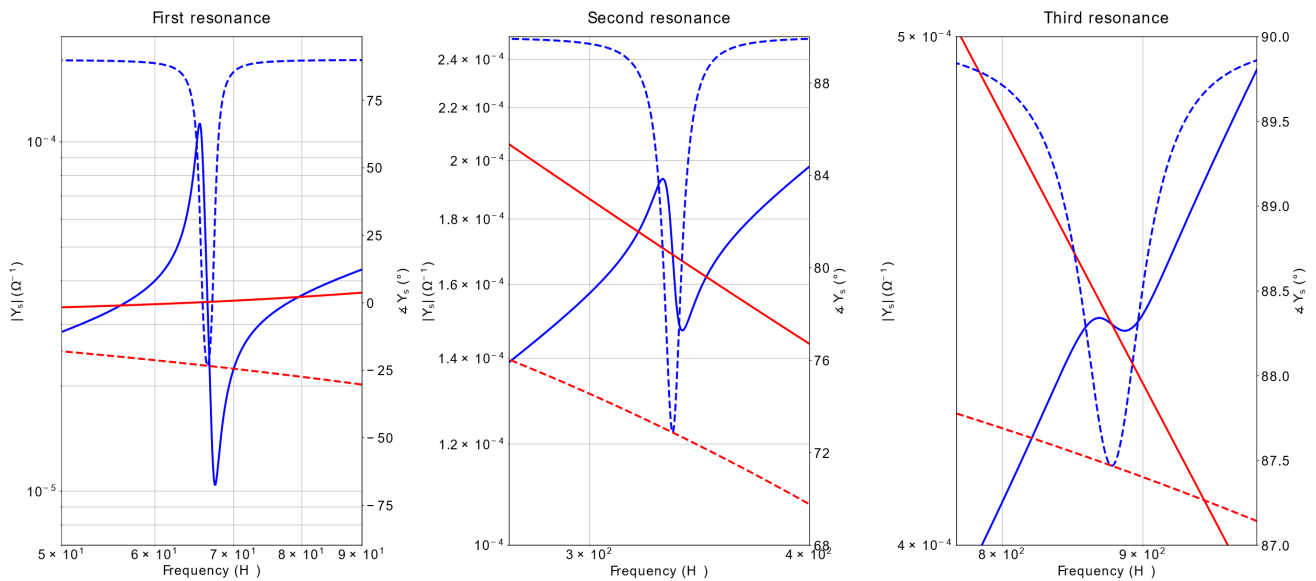


Figure 3. The complex conjugate of the load admittance (red) and source admittance (blue) for the first, second, and third resonant frequencies. Continuous lines correspond to the magnitude, while dashed lines represent the admittance phase.

Figure 3 presents the frequency responses of the complex conjugate for the three load admittances, together with the source admittance. As stated by the MPTT, the complex conjugate of the load must be equal to the source inductance, as evidenced in Figure 3. However, although the MPTT is verified at each resonant frequency, in the vicinity this condition does not hold, which leads to admittance mismatch and reduction of the extracted power. Furthermore, the three loads cannot be implemented simultaneously, meaning that the power generated at higher resonances is normally not harvested.

METHODOLOGY

As shown in the previous section, the computation of the optimum load of a PEH presents an instability problem if the maximum power transfer theorem is directly applied. Therefore, as an alternative method, the computation of the optimum load through the solution of an optimization problem is proposed. The problem is formulated as follows: Find the poles and zeros of a n^{th} order transfer function ($Y(s)$) that minimize the integral of the mean quadratic error of $Y(s)$ with the admittance presented in equation (2). This problem is presented mathematically in equation (3), where the non-negative restriction on the poles is imposed to attain BIBO stability, f_c is the maximum frequency considered and $Y(s)$ is equal to $\prod_{i=1}^n (s + z_i) / \prod_{i=1}^n (s + p_i)$.

$$\begin{aligned} \min \int_0^{2f_c} \|Y(s) - Y_L\|_2^2 ds \\ \text{s.t. } R(p_i) \leq 0 \\ z_i, p_i \in C \end{aligned} \quad (3)$$

Given that the optimization problem presented in equation (3) is not convex (given that $Y(s)$ is the ratio of two functions), the implementation of a heuristic technique is preferred. Therefore, the Particle Swarm Optimization (PSO) method is selected due to the simplicity of its implementation. It should be noted that this study uses a variation of the original method presented in Liu and Lin (2007) and Rao (2009), given the constrained nature of the problem through a penalty function approach. The steps of the PSO algorithm are listed below:

1. Generate the particle population
2. Compute the penalty objective function $F(X)$. This is performed by using equation (5), where $f(X)$ is the original objective function in equation (3) and $H(X)$ and $C(i)$ are a penalty factor and a dynamical penalty value (dependent on the iteration number i), respectively. The expression of $H(X)$ and $C(i)$ are presented in equations (6) and (7), respectively, where $q_i(X) = \max\{0, g_i(X)\}$, $\gamma(q_i(X)) = 1$ if $q_i(X) \leq 1$ and 0 otherwise, and $\theta(q_i(X))$ is presented in equation (8).

$$F(X) = f(X) + C(i) H(X) \quad (4)$$

$$H(X) = \sum_{i=1}^m \left[\theta(q_i(X)) \cdot q_i(X)^{\gamma(q_i(X))} \right] \quad (5)$$

$$C(i) = (c_i^{\wedge}) \quad (6)$$

$$\theta(q_i(X)) = a \cdot \left(1 - \frac{1}{e^{q_i(X)}} \right) + b \quad (7)$$

3. Calculate the velocity of each particle and the new position. This is performed with equations (9) and (10) presented below.

$$V_j^{i+1} = \theta V_j^i + c_1 r_1 (P_{best,j} - X_j) + c_2 r_2 (G_{best,j} - X_j) \quad (8)$$

$$X_j^{i+1} = X_j^i + V_j^{i+1} \quad (9)$$

4. If the convergence criterion is met (which can be stated as $conv < conv_0$, where $conv$ is the magnitude difference between the highest and the lowest individual in the population at each iteration, and $conv_0$ is the difference computed after the generation of the swarm) or the maximum iteration number is achieved, the algorithm finishes. It should be pointed out that, for every iteration, the best individual in the population and its objective function value were stored and compared with other iterations.

RESULTS

The algorithm presented in the previous section was computed several times for different values of n to compare the results and verify if increasing n improves the value of the objective function. Also, an unconstrained implementation of the PSO algorithm was implemented and used for comparison. The results are presented in Table 2. It is clear from the table values that the lowest objective function with stable poles was obtained at the third computation, considering a 7th-degree transfer function as a model. In this case, the zeros and poles of the model were real. The transfer function of the best solution is presented in equation (10) and its frequency response is presented in Figure 4. Finally, the implementation of the PSO algorithm is presented in Appendix 1 using the Python language

$$Y(s) = \frac{(s - 9,3 \cdot 10^4) (s - 9,17 \cdot 10^4) (s - 1,04 \cdot 10^5) (s + 6,36 \cdot 10^4) (s + 1,98 \cdot 10^4) (s_1 - 1,81 \cdot 10^2) (s + 5,22 \cdot 10^4)}{(s + 1,46 \cdot 10^5) (s + 6,81 \cdot 10^4) (s + 1,75 \cdot 10^5) (s + 1,57 \cdot 10^5) (s + 1,69 \cdot 10^5) (s + 7,01 \cdot 10^4) (s + 2,33 \cdot 10^5)} \quad (10)$$

Tabla 2. Objective function values obtained from the applications of the PSO algorithm.

n	1 st computation		2 nd computation		3 rd computation	
	f_{obj} value	unstable p_i	f_{obj} value	unstable p_i	f_{obj} value	unstable p_i
7	$5,3692 \cdot 10^{-7}$	Yes	$4,7788 \cdot 10^{-7}$	Yes	$5,8271 \cdot 10^{-7}$	No
8	$2,8908 \cdot 10^{-5}$	No	$2,3234 \cdot 10^{-5}$	No	$3,9975 \cdot 10^{-5}$	No
16	$4,2431 \cdot 10^{-5}$	No	$4,4796 \cdot 10^{-5}$	No	$6,8842 \cdot 10^{-5}$	No
20	$5,7923 \cdot 10^{-5}$	No	$1,4718 \cdot 10^{-5}$	No	1.641110^{-5}	No

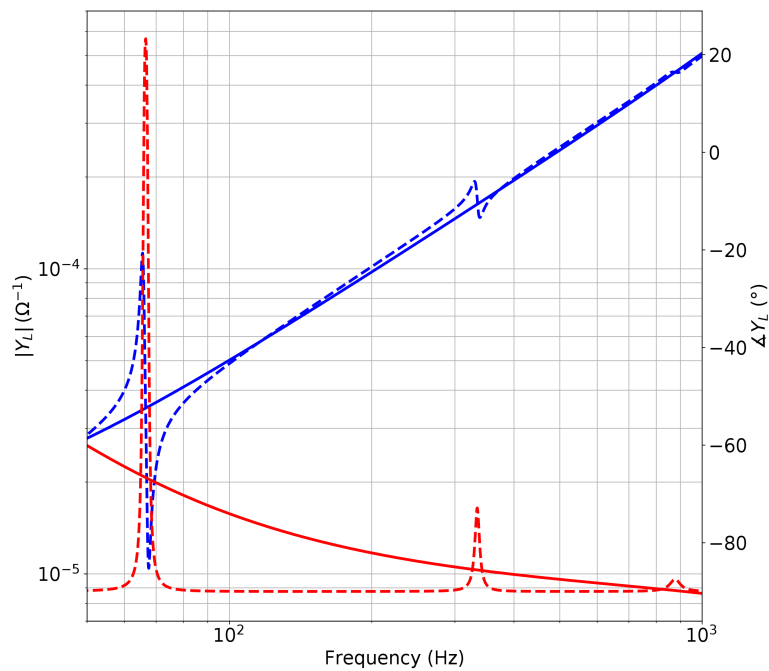


Figure 4. Frequency response of the best-found solution. Magnitude (blue) and phase (red). The dashed lines correspond to the same values of the admittance obtained through the MPT.

CONCLUSION

In this study, the computation of the model parameters of a stable transfer function that minimizes the difference between this model and the maximum power transfer admittance for a piezoelectric energy harvester has been presented. These model parameters have been obtained through the implementation of the PSO method, which has shown a low convergence for the objective function with a value of $5,8271 \cdot 10^{-7} \Omega^{-2}$. These results suggest a low dependence of the minimum objective function value on the model degree, matching the degrees of the obtained model with the admittance from the harvester. Finally, for this application, the unconstrained objective function provided better results, in terms of objective function values, than its constrained counterpart. For this reason, the exploration of other heuristics is proposed, as it can lead to better results.

FUNDING

This research was part of the project entitled “Desarrollo de un sistema de recolección de energía (Energy Harvester) basado en el efecto piezoeléctrico”, which was funded by the Corporación Nacional de Educación Superior CUN.

REFERENCES

- Bowden, J. A., Burrow, S. G., Cammarano, A., Clare, L. R., & Mitcheson, P. D. (2015). Switched-mode load impedance synthesis to parametrically tune electromagnetic vibration energy harvesters. *IEEE/ASME Transactions on Mechatronics*, 20(2), 603–610. <https://doi.org/10.1109/TMECH.2014.2325825>
- Cammarano, A., Neild, S. A., Burrow, S. G., Wagg, D. J., & Inman, D. J. (2014). Optimum resistive loads for vibration-based electromagnetic energy harvesters with a stiffening nonlinearity. *Journal of Intelligent Material Systems and Structures*, 25(??), 1757–1770. <https://doi.org/10.1177/1045389X14523854>

- Liu, J.-L., & Lin, J.-H. (2007). Evolutionary computation of unconstrained and constrained problems using a novel momentum-type particle swarm optimization. *Engineering Optimization*, 39(3), 287–305. <https://doi.org/10.1080/03052150601131000>
- Ocalan, M., Pabon, H., Chang, S., & Lang, J. (2017). *Non-stationary Multi-frequency Vibration Energy Harvesting with Tunable Electrical Impedance* (Patent No. US 9,595,893 B2).
- Rao, S. S. (2009). *Engineering optimization theory and practice / Singiresu S. Rao*. <http://search.ebscohost.com/login.aspx?direct=true&db=cat01040a&AN=pujbc.856901&site=eds-live>
- Safaei, M., Sodano, H. A., & Anton, S. R. (2019). A review of energy harvesting using piezoelectric materials: State-of-the-art a decade later (2008-2018). *Smart Materials and Structures*, 28(11). <https://doi.org/10.1088/1361-665X/ab36e4>
- Todoaro, M. T., Guido, F., Mastronardi, V., Desmaele, D., Epifani, G., Algieri, L., & de Vittorio, M. (2017). Piezoelectric MEMS vibrational energy harvesters: Advances and outlook. *Microelectronic Engineering*, 183–184, 23–36. <https://doi.org/10.1016/j.mee.2017.10.005>
- Uchino, K. (2018). Piezoelectric Energy Harvesting Systems—Essentials to Successful Developments. *Energy Technology*, 6(5), 829–848. <https://doi.org/10.1002/ente.201700785>
- Yang, Y., & Tang, L. (2009). Equivalent Circuit Modeling of Piezoelectric Energy Harvesters. *Journal of Intelligent Material Systems and Structures*, 20(??), 2223–2235. <https://doi.org/10.1177/1045389X09351757>

APPENDIX 1: IMPLEMENTATION OF THE PSO ALGORITHM

```
def integrand(wn,X,a,Y_obj):  
    Yzp = 1  
    for k in range(a):  
        Yzp = (X[k+1j*wn]*(np.conj(X[k])+1j*wn))*Yzp  
    for k in range(X.size-a):  
        Yzp = Yzp/((X[k+a]+1j*wn)*(np.conj(X[k+a])+1j*wn))
```

```
return np.abs(Yzp-Y_obj(wn))**2
def obj_func(fc,X,a_int,Y_obj,a_pso,b_pso):
f = integral.quad(integrand,0,2*np.pi*fc,args=(X,a_int,Y_obj))[0]
g_i = np.concatenate((np.zeros(a_int),-np.real(X[a_int:])),axis=0)
q_i = np.maximum(g_i,np.zeros(X.size))
gamma = np.empty(X.size)
for k in range(X.size):
if q_i[k]<=1:
gamma[k] = 1
else:
gamma[k] = 2
theta = a*(1-1/np.exp(q_i))+b
H = np.sum(theta*q_i**gamma)
return f,H
n_poles, n_zeros = 20, 20
N = 600
c1, c2 = 2, 2
a, b = 150, 10
c, alpha = 0.5, 2
theta_max, theta_min = 1, 0.4
i_max = 250
X = 10000*(np.random.rand(N,int((n_poles+n_zeros)/2))
+1j*np.random.rand(N,int((n_poles+n_zeros)/2))-0.5j)
V = np.zeros((N,int((n_poles+n_zeros)/2)))
F = np.empty(N)
P_best = 10e12*np.ones(N)
X_p_best = np.empty((N,int((n_poles+n_zeros)/2)))
G_best = 10e12
X_g_best = np.empty(int((n_poles+n_zeros)/2))
```

```
i = 0
conv_circle = np.max(np.abs(X))- np.min(np.abs(X))
conv_circle_0 = np.max(np.abs(X))- np.min(np.abs(X))
while i<=i_max and conv_circle>0.1*conv_circle_0:
for k in range(N):
fopt, h = obj_func(1000,X[k],int(n_zeros/2),YL_n,a,b)
C_i = (c*i)**alpha
F[k] = fopt + C_i*h
if F[k]<P_best[k]:
P_best[k] = F[k]
X_p_best[k] = X[k]
if F[k]<G_best:
G_best = F[k]
X_g_best = X[k]
theta = theta_max - i*(theta_max-theta_min)/i_max
r1 = np.random.rand()
r2 = np.random.rand()
V = theta*V + c1*r1*(X_p_best-X) + c2*r2*(X_g_best-X)
X = X + V
conv_circle = np.max(np.abs(X))- np.min(np.abs(X))
i = i+1
```

